

## $(n, xn)$ cross sections on $^{56,57}\text{Fe}$

Alexandru Negret<sup>1,a</sup>, Catalin Borcea<sup>1</sup>, Philippe Dessagne<sup>2</sup>, Maëlle Kerveno<sup>2</sup>, Nikolay Nankov<sup>3</sup>, Adina Olacel<sup>1</sup>, Arjan Plompen<sup>3</sup>, Charoula Rouki<sup>3</sup>, Mihaela Sin<sup>4</sup>, and Mihai Stanoiu<sup>1</sup>

<sup>1</sup> Horia Hulubei National Institute for Physics and Nuclear Engineering, Măgurele, Romania

<sup>2</sup> Unistra, CNRS, IPHC, Strasbourg, France

<sup>3</sup> European Commission, Joint Research Centre - Geel, Belgium

<sup>4</sup> University of Bucharest, Faculty of Physics, Măgurele, Romania

**Abstract.** The Gamma Array for Inelastic Neutron Scattering (GAINS) operated at the Geel Linear Accelerator (GELINA) neutron source was used to measure  $(n, xn)$  cross sections on  $^{56,57}\text{Fe}$  reaching a level of uncertainty of the order of 5%. Serious difficulties arise in case of the  $^{57}\text{Fe}$  isotope from the fact that the first excited level has an energy of only 14 keV and its decay could not be observed. Therefore a delicate combination of experimental and theoretical approaches have to be used to infer the inelastic cross section. The particularities of the two measurements are presented concentrating on the approaches allowing us to overcome specific problems in each case.

### 1. Introduction

Iron is undoubtedly one of the most important structural materials, largely used in the architecture of the large scale nuclear facilities. It has four stable isotopes:  $^{54}\text{Fe}$  (natural abundance 5.85(11)%),  $^{56}\text{Fe}$  (91.75(11)%),  $^{57}\text{Fe}$  (2.12(3)%), and  $^{58}\text{Fe}$  (0.28(1)%) [1]. Inelastic scattering represents a major mechanism for slowing down neutrons and consequently the neutron inelastic cross sections of iron are a major ingredient in the design of nuclear facilities.

Therefore the program of measuring neutron inelastic cross section for structural materials of importance for the development of the fourth generation of nuclear reactors currently ongoing at the Geel Linear Accelerator (GELINA) [2–10] facility of the Joint Research Centre of the European Commission (EC-JRC) from Geel, Belgium included several experiments on iron isotopes. The results of two such measurements on the major isotope  $^{56}\text{Fe}$  were published recently [7] while the data gathered during a recent experiment investigating the neutron inelastic scattering on  $^{57}\text{Fe}$  are currently under analysis and the results should become available soon. Finally, an investigation of the other minor isotope  $^{54}\text{Fe}$  is foreseen to start before the end of 2016.

This paper describes the experiments performed on the major isotope  $^{56}\text{Fe}$  and on the minor one  $^{57}\text{Fe}$  emphasizing the specificities of each measurement, the experimental challenges and the solutions we applied in order to obtain high-quality results.

We note that, although  $^{57}\text{Fe}$  is less abundant than  $^{54}\text{Fe}$ , the investigation of this isotope is of particular interest for two reasons: First, due to the particular structure of the even-even iron stable isotopes, the low-energy ( $E_n \leq 850$  keV) neutron inelastic scattering on iron can only occur on  $^{57}\text{Fe}$ : the first excited levels of  $^{54}\text{Fe}$  and

$^{56}\text{Fe}$  lie at 1408 and 847 keV, respectively while  $^{57}\text{Fe}$  has four excited levels below 850 keV [11–13]. Second, at high neutron energies ( $E_n \geq 7.5$  MeV) the cross sections of the  $^{56}\text{Fe}(n, n')^{56}\text{Fe}$  reaction determined using  $\gamma$  spectroscopy techniques and a  $^{nat}\text{Fe}$  target (as it is our case) are “contaminated” by the  $^{57}\text{Fe}(n, 2n)^{56}\text{Fe}$  reactions occurring on the minor isotope. Figure 1 shows the low-excitation energy level schemes of  $^{56,57}\text{Fe}$ .

The second section gives a short overview of the experimental setup. The most extended section, the third one, describes the particular difficulties specific to each of the two measurements. The fourth section is dedicated to the experimental results. The  $^{56}\text{Fe}$  results were already reported in Ref. [7] while for  $^{57}\text{Fe}$  they are of a preliminary nature. The last section concludes the paper.

### 2. Experimental setup and analysis technique

The experimental setup consisted of the neutron source GELINA (Geel Linear Accelerator) and the GAINS (Gamma Array for Inelastic Neutron Scattering) spectrometer. It was already described several times (see, e.g., Ref. [6] or [9] and the references therein) and therefore we will only give here a short overview for completeness.

GELINA is a pulsed, white neutron source providing significant flux for neutron energies ranging from  $\approx 70$  keV to  $\approx 18$  MeV. Each neutron pulse has a duration of  $\approx 1$  ns and is produced together with a very intense  $\gamma$  flash. The neutron bursts fly along a 200-m evacuated beam line. As the neutron energy is determined using the time-of-flight method, the combination between the long flight path and the very good time resolution of the source allows high-resolution measurements. Along the 200-m beam line the neutron flux is collimated to a beam-like shape and filtered in order to reduce the relative  $\gamma$ -flash to neutron intensity.

<sup>a</sup> e-mail: alnegret@tandem.nipne.ro

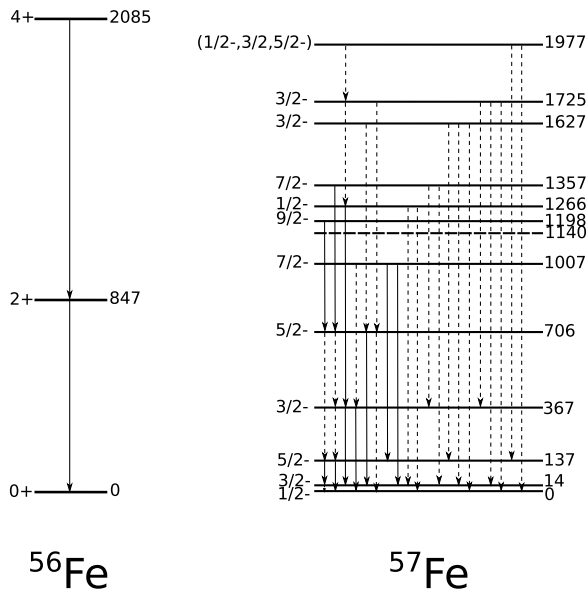


**Figure 1.** Low excitation energy evaluated level schemes of  $^{56,57}\text{Fe}$  taken from Refs. [11, 12]. The excitation functions of the transitions shown with continuous lines were determined during our measurements.

GAINS consists of 12 HPGe (High-Purity Germanium) detectors placed at backward angles representing the nodes of the 2nd and 4th order Legendre Polynomials and pointing to the sample. This special choice of the detection angles allows angular integration of the differential cross sections. Not all detectors were operational during the multiple measurements dedicated to  $^{56,57}\text{Fe}$ .

The neutron flux was determined using a  $^{235}\text{U}$  fission chamber placed before GAINS and the sample. In the experimental cabin the collimated neutron beam has a diameter of 6.1 cm. All samples used in the current measurements were larger than the beam.

Our experimental method uses  $\gamma$  spectroscopy to detect the  $\gamma$  rays emitted following the inelastic scattering reactions and the time of flight method to determine the neutron energy. The primary experimental results are the  $\gamma$ -production cross sections. The level cross sections and the total inelastic cross sections can be subsequently calculated assuming the level scheme of the investigated nucleus from an external source. We commonly use the evaluated level schemes from ENSDF (Evaluated Nuclear Structure Data File).

### 3. Experimental particularities and difficulties

For the major isotope  $^{56}\text{Fe}$ , the measurement required extreme precision, especially for the first transition (847 keV). This transition may be contaminated by the 844-keV  $\gamma$ -ray from  $^{27}\text{Al}$  or the specific triangle-shaped background produced by the inelastic scattering of neutrons on  $^{76}\text{Ge}$  nuclei from the detector crystals.

In case of  $^{57}\text{Fe}$ , the main difficulty arose from the particular structure of this nucleus: the first excited level lies at  $E_x = 14.4$  keV (see Fig. 1) and has a half life of  $T_{1/2} = 98.3(3)$  ns. It decays through a transition of 14.4 keV with a conversion coefficient  $\alpha = 8.5(3)$  [12]. The detection of such a small-energy  $\gamma$ -ray with the

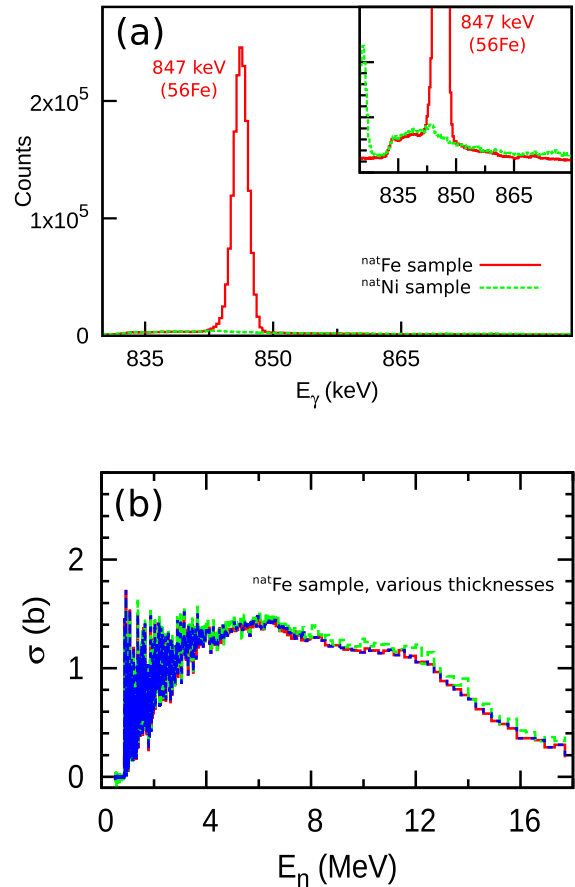


**Figure 2.** Various checks performed to check the consistency of the  $^{56}\text{Fe}$  data. (a)  $\gamma$  spectra around  $E_x = 847$  keV obtained during the scattering of neutrons on a  $^{nat}\text{Fe}$  (red line) and a  $^{nat}\text{Ni}$  (green line) sample. (b) 847-keV  $\gamma$ -production cross section obtained with  $^{nat}\text{Fe}$  samples of various thicknesses: 1 mm (green line), 3 mm (blue line) and 4 mm (red line).

large-volume HPGe detectors of GAINS represented the main challenge of this measurement.

#### 3.1. Particularities of the $^{56}\text{Fe}$ measurement

In order to reach the level of reliability required for the  $^{56}\text{Fe}$  data, we dedicated two measuring campaigns to this isotope.

During the first campaign we gathered (for about two months) the data required to generate low-uncertainty  $\gamma$ -production cross sections for several transitions. A  $^{nat}\text{Fe}$  sample with a thickness of 3 mm was used. The results of the data analysis were published in Ref. [7] and made available for the EXFOR (Exchange Format) database.

But before releasing these results, a second measuring campaign was dedicated to several consistency checks: we measured under identical conditions several samples (Al – one day, Ni – one week, Pb – one week) and an empty frame (one week) in order to check the background conditions in the excitation energy region around  $E_\gamma = 847$  keV. Also, we measured two additional  $^{nat}\text{Fe}$  samples with thicknesses of 1 mm (2 weeks) and 4 mm (3 weeks) in order to make sure that the corrections we make for the attenuation of  $\gamma$ -rays and the multiple scattering of neutrons in the sample are consistent. Figure 2 illustrates these investigations insuring the robustness of our results.

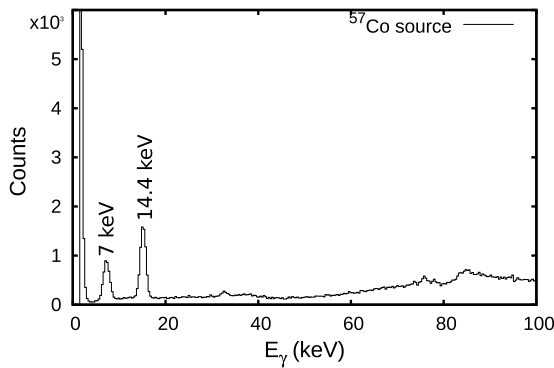


**Figure 3.** Spectrum of a  $^{57}\text{Co}$  source collected with one of the GAINS detectors during the  $^{57}\text{Fe}(n, n')$  experiment.

### 3.2. Particularities of the $^{57}\text{Fe}$ measurement

The first practical difficulty of the  $^{57}\text{Fe}$  measurement was the target itself. As this is a minor isotope, the procurement of 20 grams of enriched material (as it was our case) was an issue in terms of cost and availability. We used an iron sample with a 90.5(3)% enrichment in  $^{57}\text{Fe}$ . It had the approximative shape of a cylinder with the diameter larger than the beam and a height of  $\approx 0.67$  mm but with a rounding at the edges. In order to estimate the areal density we weighted and measured the area of the sample. Then, due to the specific shape (rounded edges), we estimated that the real mass irradiated by neutrons is larger by 3(1)%. This resulted in an effective areal density of the sample of  $0.542(5)$  g/cm $^2$ .

Several precautions and small adaptations of the acquisition system had to be applied in order to deal with the issue of the 14-keV transition in  $^{57}\text{Fe}$ .

First of all, in the common configuration the digitized acquisition system is set to acquire data for about 24  $\mu\text{s}$  for each beam burst. This corresponds to neutron energies larger than  $\approx 0.4$  MeV for the 200-m flight path and for most nuclei this is sufficient because the first excited level lies at higher energies. However, in case of  $^{57}\text{Fe}$  this is not the case: as already mentioned in the introduction, the neutron inelastic scattering on  $^{57}\text{Fe}$  occurs at even smaller energies and therefore we had to double the time range of data taking for each beam burst. This rose concerns with regard to the possible dead time due to the longer time required to transfer the data from the digitizer cards to the acquisition computers. After several checks we concluded that, due to the low counting rate (of the order of 10 counts/s for each detector), the additional dead time is negligible.

Further, we had to adapt GAINS to gain sensitivity for very small  $\gamma$  energies: we removed the absorbers usually used in front of the HPGe detectors. Also, we lowered as much as possible the trigger levels on the CFD (Constant Fraction Discriminator) signals used to trigger the digitizers as well as the software triggers used on the analysis of the digitized HPGe signals. Figure 3 displays the result of these changes: the shown spectrum was taken using a  $^{57}\text{Co}$  calibration source (producing the same 14-keV  $\gamma$  ray following  $\beta$  decay to  $^{57}\text{Fe}$ ). Not only the 14-keV peak but also a 7-keV X ray are visible.

Unfortunately, the above described effort was not fully successful: although Fig. 3 shows that GAINS was well prepared to detect very low-energy  $\gamma$  rays, during the

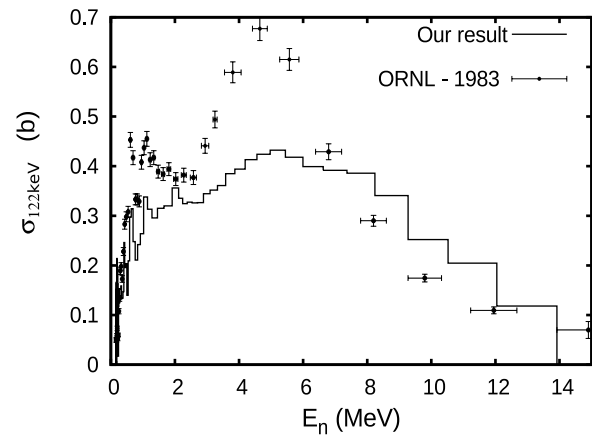


**Figure 4.** Production cross section of the 122-keV  $\gamma$  ray excited in the  $^{57}\text{Fe}(n, n\gamma)^{57}\text{Fe}$  reaction. Our preliminary result is compared with the one from Ref. [14].

$^{57}\text{Fe}(n, n\gamma)$  experiment this region was affected by a huge background. This prevented the detection of the first transition in  $^{57}\text{Fe}$  making the data interpretation much more difficult. We can speculate that the large background at low excitation energies is due to the collection in the detector crystals of the energy deposited by recoiling Ge nuclei following elastic scattering of neutrons.

## 4. Results

As the results of the neutron inelastic scattering experiment on  $^{56}\text{Fe}$  were already published [7], we will not show them again. We emphasized in the previous section the multitude of consistency checks performed during this experiment to insure the robustness of the results.

The  $^{57}\text{Fe}$  measurement rose serious difficulties due to the fact that our setup was not capable of detecting the first transition. Unfortunately, as it is clear from Fig. 1, this transition collects a significant part of the strength excited in the inelastic scattering. Not knowing experimentally this strength prevents direct determination of the total inelastic cross section on  $^{57}\text{Fe}$ .

However, the  $^{57}\text{Fe}$  measurement allowed us to determine the  $\gamma$ -production cross sections for other 10 transitions. Figure 4 displays the preliminary result obtained for the decay of the second excited state to the first one (137 keV to 14 keV). It is compared with previous data obtained at Oak Ridge National Laboratory and reported in Ref. [14] and significant differences are visible. As this is a work-on-progress, it is premature to comment on these differences.

## 5. Conclusions and perspectives

The conclusion regarding  $^{56}\text{Fe}$  is that the data we presented in Ref. [7] are reliable and of good quality. The uncertainty of the strongest transitions and on the total inelastic cross section is around 5% for incident energies below 10 MeV and rises slowly at higher neutron energies.

For the case of  $^{57}\text{Fe}$  a interplay between our experimental results and the theory will be necessary in order to generate the total inelastic cross section: We will employ the well-known reaction codes TALYS [15] and EMPIRE [16] to fit the  $\gamma$ -production cross sections determined experimentally for the  $(n, n')$  and  $(n, 2n)$

reaction channels. Further, gaining confidence that all parameters used by the theoretical models are tuned to describe correctly the interaction between neutrons and the  $^{57}\text{Fe}$  isotope, we will use the theoretically calculated  $\gamma$ -production cross section for the 14-keV transition to generate the total inelastic cross section.

In conclusion, the experimental program ongoing at GELINA addressing the neutron inelastic cross sections on iron isotopes produced high precision results for the major isotope  $^{56}\text{Fe}$ . Following a more delicate experiment, results on  $^{57}\text{Fe}$  will become available during the next months, while a measurement on the third significant isotope  $^{54}\text{Fe}$  is scheduled before the end of 2016.

The authors thank the team of operators of the GELINA facility for the preparation of the neutron beam and to the technical staff of EC-JRC Geel for their support during the data taking campaign. This work was partially supported by the European Commission through the CHANDA (EURATOM contract number FP7-605203) project. Finally, we acknowledge the support provided through the EUFRAT transnational access program to the EC-JRC Geel experimental facilities.

## References

- [1] J. Meija et al., *Pure and Appl. Chem.* **88**, 293–306 (2016)
- [2] L.C. Mihailescu, C. Borcea, A.J. Koning, A.J.M. Plompen, *Nucl. Phys. A* **786**, 1–23 (2007)
- [3] L.C. Mihailescu, C. Borcea, A.J. Koning, A. Pavlik, A.J.M. Plompen, *Nucl. Phys. A* **799**, 1–29 (2008)
- [4] C. Rouki, P. Archier, C. Borcea, C. De Saint Jean, J.C. Drohe, S. Kopecky, A. Moens, N. Nankov, A. Negret, G. Noguere, A.J.M. Plompen, and M. Stanoiu, *Nucl. Instrum. Methods Phys. Research A* **672**, 82 (2012)
- [5] A. Negret, C. Borcea, D. Bucurescu, D. Deleanu, Ph. Dessagne, D. Filipescu, D. Ghita, T. Glodariu, M. Kerveno, N. Marginean, R. Marginean, C. Mihai, S. Pascu, A.J.M. Plompen, T. Sava, and L. Stroe, *Phys. Rev. C* **88**, 034604 (2013)
- [6] A. Olacel, C. Borcea, Ph. Dessagne, M. Kerveno, A. Negret, and A.J.M. Plompen, *Phys. Rev. C* **90**, 034603 (2014)
- [7] A. Negret, C. Borcea, Ph. Dessagne, M. Kerveno, A. Olacel, A.J.M. Plompen, and M. Stanoiu, *Phys. Rev. C* **90**, 034602 (2014)
- [8] A. Negret, L.C. Mihailescu, C. Borcea, Ph. Dessagne, K.H. Guber, M. Kerveno, A.J. Koning, A. Olacel, A.J.M. Plompen, C. Rouki, and G. Rudolf, *Phys. Rev. C* **91**, 064618 (2015)
- [9] M. Nyman, F. Belloni, D. Ichinkhorloo, E. Pirovano, A.J.M. Plompen, and C. Rouki, *Phys. Rev. C* **93**, 024610 (2016)
- [10] C. Borcea et al., *These proceedings* (2016)
- [11] H. Junde, H. Su, and Y. Dong, *Nucl. Data Sheets* **112**, 1513 (2011)
- [12] M.R. Bhat, *Nucl. Data Sheets* **85**, 415 (1998)
- [13] Y. Dong and H. Junde, *Nucl. Data Sheets* **121**, 1 (2014)
- [14] Z.W. Bell, J.K. Dickens, D.C. Larson, and J.H. Todd, *Nucl. Sci. Eng.* **84**, 12 (1983)
- [15] A.J. Koning, S. Hilaire, and M.C. Duijvestijn, in *Proceedings of the International Conference on Nuclear Data for Science and Technology – ND2004, September 26 – October 1, 2004, Santa Fe, USA*, edited by R.C. Haight, M.B. Chadwick, T. Kawano, and P. Talou (AIP Conf. Proc. 769, 2005), p. 769
- [16] M. Herman, R. Capote, B.V. Carlson, P. Oblozinsky, M. Sin, A. Trkov, H. Wienke, V. Zerkin, *Nucl. Data Sheets* **108** (2007)